CBN 97–01
January 14, 1997

Wave Analysis for Finding Isolated Steering, Quadrupole, and Skew Quadrupole Errors

David Sagan

Abstract

The program K_FIT has been modified to have the ability to extract the locations and strengths of isolated steering, quadrupole and skew quadrupole errors. The mathematics behind the wave analysis is presented along with example analyses of data.

1 Orbit Analysis

Given a steering error that is isolated, so that there are no other steering errors near it, then it is possible to find the location and strength of the kick error by taking an orbit measurement. This is shown schematically in figure 1. An isolated steering error is at s_k. On either side of the steering error the orbit $x(s)$ must be a "free wave" which can be written as

$$x(s) = \begin{cases} \sqrt{\beta(s)}\left[\lambda_a \sin\phi(s) + \rho_a \cos\phi(s)\right] & s < s_k \\ \sqrt{\beta(s)}\left[\lambda_b \sin\phi(s) + \rho_b \cos\phi(s)\right] & s > s_k \end{cases} . \tag{1}$$

Eq. (1) is linear in the unknowns λ and ρ. Given regions "A" and "B" on either side of s_k (cf. figure 1), λ_a and ρ_a can be determined by a linear least squares fit to the data from region A. Similarly, λ_b and ρ_b are determined by a fit with the B region data.

Once the coefficients are determined we can "extend" the waves into the area between the regions to find the kick. To simplify the analysis we choose a new reference orbit x_{ref} by

$$x_{ref}(s) \equiv \sqrt{\beta(s)}\left[\lambda_a \sin\phi(s) + \rho_a \cos\phi(s)\right] \tag{2}$$

The offset $\tilde{x} \equiv x - x_{ref}$ from the new reference is then

$$\tilde{x}(s) = \begin{cases} 0 & s < s_k \\ \sqrt{\beta(s)}\left[\lambda_{ba} \sin\phi(s) + \rho_{ba} \cos\phi(s)\right] & s > s_k \end{cases} . \tag{3}$$

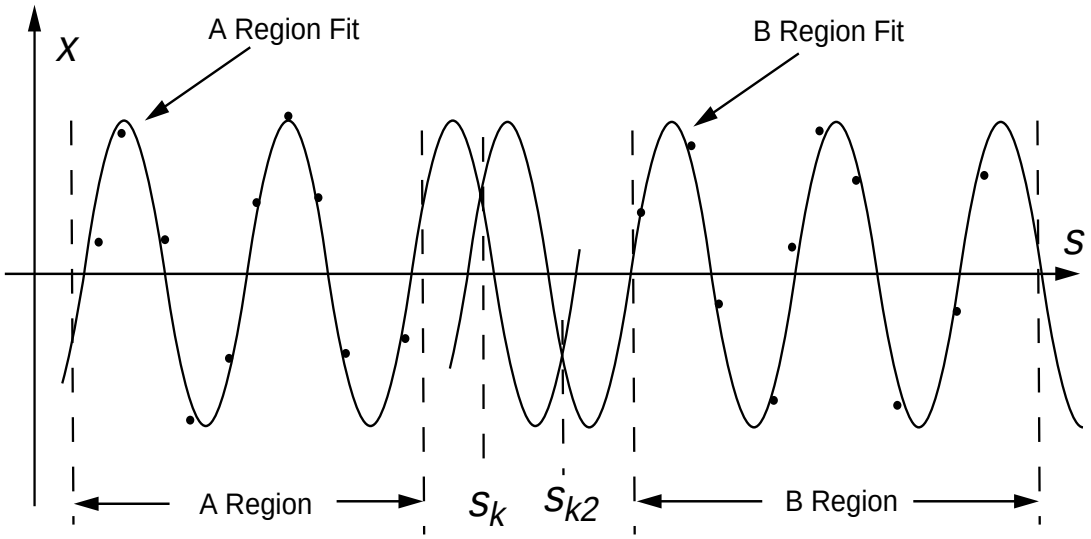

Figure 1: Schematic diagram of the analysis to find a steering error at s_k. An orbit measurement in regions A and B is fit to free waves and the fits are propagated into the area between the regions. The possible kicker locations are where the waves cross at s_k and s_{k2}

where

$$\begin{aligned} \lambda_{ba} &\equiv \lambda_b - \lambda_a \ , \\ \rho_{ba} &\equiv \rho_b - \rho_a \ . \end{aligned} \tag{4}$$

Since $\tilde{x}(s)$ must be continuous, the kick error must be at a place where the waves intersect (cf. figure 1). Thus, from Eq. (3), the phase ϕ_k at the kick point is given by

$$\tan \phi_k = -\frac{\rho_{ba}}{\lambda_{ba}} \ , \tag{5}$$

The solutions to Eq. (5) are a series of phases spaced π apart. If regions A and B are close enough together then only 1 solution will land in–between and the correct kicker phase can be determined unambiguously.

The kick magnitude $\Delta x'$ is obtained from differentiating Eq. (3)

$$\sqrt{\beta_k}\, \Delta x' = \lambda_{ba} \cos \phi_k - \rho_{ba} \sin \phi_k \ . \tag{6}$$

Eq. (6) can be put in a more transparent form using Eq. (5)

$$\sqrt{\beta_k}\, \Delta x' = \pm A_{ba} \ , \tag{7}$$

where

$$A_{ba}^2 \equiv \lambda_{ba}^2 + \rho_{ba}^2 \,. \tag{8}$$

For computations Eq. (6) is to be preferred since it gives the sign of the kick.

An example of an orbit analysis is shown in figure 2. The data to be analyzed is a horizontal difference orbit which was obtained by Stu Peck by taking a orbit under zero corrector conditions and then changing the horizontal tune by about $-6\,\mathrm{kHz}$. Plotted on the x–axis in figure 2 is the detector index. In order to be able to analyze errors near L0 the data has been extended past L0 by adding 100 to the index. Thus, for example, 32 and 132 both correspond to the 32W detector.

Shown in figure 2 are the residuals which are obtained by taking the difference orbit and subtracting off the two fits for the A and B regions. At the bottom of the figure is the results of the analysis. IX_A1 and IX_A2 are the indices for the left and right ends of region A. Similarly IX_B1 and IX_B2 delimit region B. The fits are done using the subroutine SVDFIT from Numerical Recipes[3]. For both regions a figure of merit for the goodness of the fit, σ_a/A_a and σ_b/A_b, is defined by the formula*

$$\frac{\sigma}{A} \equiv \frac{\sqrt{\sigma_\lambda^2 + \sigma_\rho^2}}{A} \,, \tag{9}$$

where the amplitudes A_a and A_b for the regions are given by

$$A \equiv \sqrt{\lambda^2 + \rho^2} \,. \tag{10}$$

σ_λ and σ_ρ are computed Using Eq. 15.4.12 from Numerical Recipes with the variances $\sigma_{i,a}$ and $\sigma_{i,b}$ of the individual data points in regions A and B are taken to be equal to the variance between the data and the fit for that region (cf. Numerical Recipes Eq. 15.1.6 and the discussion in section 15.2):

$$\sigma_i^2 \equiv \frac{1}{N} \sum_j (x_j(data) - x_{fit}(s_j))^2 \,. \tag{11}$$

The relative uncertainty in the computed value of the kick is obtained from Eq. (7) and Eq. (10)

$$\frac{\sigma_K}{K} = \frac{\sqrt{\lambda_{ba}^2 \sigma_{\lambda ba}^2 + \rho_{ba}^2 \sigma_{\rho ba}^2}}{A_{ba}^2} \,, \tag{12}$$

where $\sigma_{\lambda ba}$ and $\sigma_{\rho ba}$ are computed from Eq. (4):

$$\begin{aligned} \sigma_{\lambda ba}^2 &= \sigma_{\lambda a}^2 + \sigma_{\lambda b}^2 \,, \\ \sigma_{\rho ba}^2 &= \sigma_{\rho a}^2 + \sigma_{\rho b}^2 \,. \end{aligned} \tag{13}$$

*For compactness repeated a and b subscripts have been dropped.

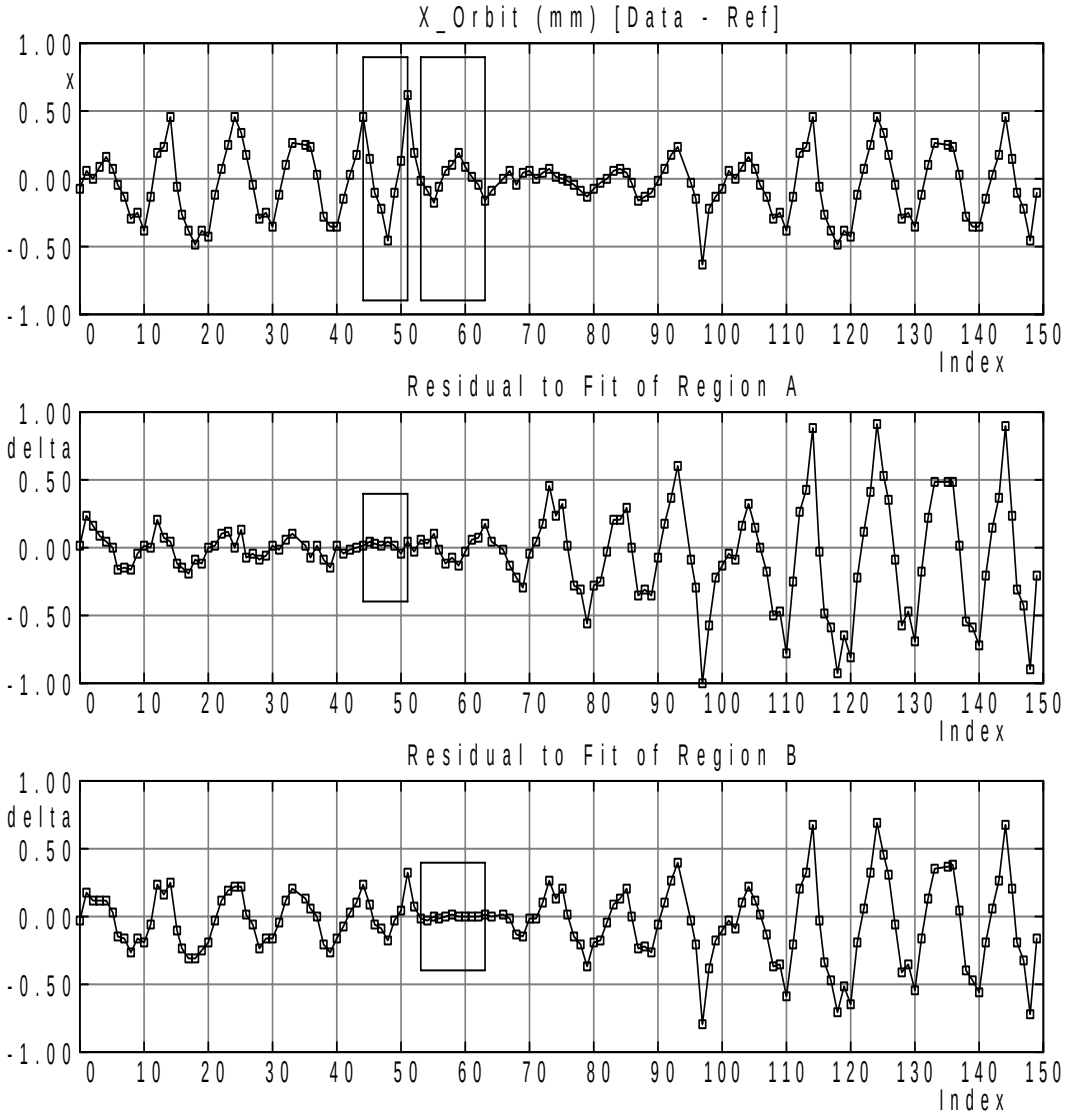

Figure 2: Wave analysis of a horizontal orbit difference

The uncertainty in ϕ_k is obtained from Eq. (5)

$$\sigma_\phi = \frac{\sqrt{\rho_{ba}^2\,\sigma_{\lambda ba}^2 + \lambda_{ba}^2\,\sigma_{\rho ba}^2}}{A_{ba}^2}\,, \tag{14}$$

In order for the error in the calculation of the kick to be small one must have

$$\frac{\sigma_K}{K},\ \sigma_\phi \ll 1\,. \tag{15}$$

From the fits to the regions $\phi_x(s_k)$ and $\sqrt{\beta_x}\Delta x''$ are computed as shown in figure 2. Only one possible kick location between detectors 52 and 53 is found that is in–between the A and B regions. Since some lattice tables only give half the ring $\phi_{ring} - \phi_k$ is also tabulated where ϕ_{ring} is the tune.

The kick found by the analysis coincides with a maximum of the orbit. There are other places on the graph where there appear to be kicks and these can be analyzed in a similar manner. These also correspond to places where there is a maximum in the orbit.

2 Beta Analysis

It is assumed that any quad errors are small and first order perturbation theory is used to obtain $\delta\beta$ — The variation of β from the reference beta. Consider the transfer matrix $\mathbf{T}_{21}$ from some point s_1 to some point s_2

$$\mathbf{T}_{21} = \begin{pmatrix} m_{11} & m_{12} \\ m_{21} & m_{22} \end{pmatrix}\,, \tag{16}$$

where m_{11} and m_{12} are given by[1]

$$\begin{aligned} m_{11} &= \sqrt{\frac{\beta_2}{\beta_1}}\Big(\cos\phi_{21} + \alpha_1\,\sin\phi_{21}\Big)\,, \\ m_{12} &= \sqrt{\beta_1\beta_2}\,\sin\phi_{21}\,, \end{aligned} \tag{17}$$

and ϕ_{21} is the phase advance from s_1 to s_2.

Let point s_1 be a point just before an isolated quad error at s_k of strength $\delta k\,l$. The transfer matrix from s_1 to a point s_2 someplace after the kick is

$$\begin{pmatrix} m_{11}+\delta m_{11} & m_{12}+\delta m_{12} \\ m_{21}+\delta m_{21} & m_{22}+\delta m_{22} \end{pmatrix} = \begin{pmatrix} m_{11} & m_{12} \\ m_{21} & m_{22} \end{pmatrix} \begin{pmatrix} 1 & 0 \\ \delta k\,l & 1 \end{pmatrix}\,, \tag{18}$$

where the m_{ij} are the unperturbed matrix elements and the δm_{ij} are the variations due to the error. Note that a positive δk represents a defocusing error. The (1,1) and (1,2) terms of Eq. (18) give

$$\begin{aligned} \delta m_{11} &= \delta k\,l\,m_{12} \\ \delta m_{12} &= 0\,. \end{aligned} \tag{19}$$

In general, β_2 at s_2 can be written as[1]

$$\beta_2 = m_{11}^2 \beta_1 - 2 m_{11} m_{12} \alpha_1 + m_{12}^2 \gamma_1 \ . \tag{20}$$

We take as the boundary condition that for $s < s_k$ the variation is 0. Thus $\delta\beta_1 = \delta\alpha_1 = \delta\gamma_1 = 0$. Using this and Eq. (19) with the variation of Eq. (20) gives

$$\delta\beta_2 = (2 m_{11} \beta_1 - 2 m_{12} \alpha_1)\, \delta k\, l\, m_{12} \ . \tag{21}$$

Using Eq. (17) in Eq. (21) gives the solution

$$\delta\beta(s) = \begin{cases} 0 & s < s_k \\ \beta(s)\beta_k \delta k\, l \sin 2(\phi(s) - \phi_k) & s > s_k \end{cases} \ . \tag{22}$$

A free beta wave thus oscillates as $2\phi(s)$ — at twice the frequency of an orbit wave. The equations used to fit the A and B regions is thus

$$\delta\beta(s) = \begin{cases} \beta(s)\Big[\lambda_a \sin 2\phi(s) + \rho_a \cos 2\phi(s)\Big] & s < s_k \\ \beta(s)\Big[\lambda_b \sin 2\phi(s) + \rho_b \cos 2\phi(s)\Big] & s > s_k \end{cases} \ . \tag{23}$$

As before, we go to a new reference so that so that the variation with respect to the new reference, $\delta\tilde{\beta}(s)$, is zero for $s < s_k$

$$\delta\tilde{\beta}(s) = \begin{cases} 0 & s < s_k \\ \beta(s)\Big[\lambda_{ba} \sin 2\phi(s) + \rho_{ba} \cos 2\phi(s)\Big] & s > s_k \end{cases} \ , \tag{24}$$

with λ_{ba} and ρ_{ba} given by Eqs. (4). Since $\delta\tilde{\beta}$ must be continuous ϕ_k is given by

$$\tan 2\phi_k = -\frac{\rho_{ba}}{\lambda_{ba}} \ , \tag{25}$$

The solutions to Eq. (25) are a series of phases spaced $\pi/2$ apart. Comparing Eq. (22) to Eq. (24) the strength of the quad error is given by

$$\begin{aligned} \beta_k\, \delta k\, l &= \lambda_{ba} \cos 2\phi_k - \rho_{ba} \sin 2\phi_k \\ &= \pm A_{ba} \ , \end{aligned} \tag{26}$$

where A_{ba} is given by Eq. (8).

Since beta measurements are seldom done nowadays the beta wave analysis has not been implemented in K_FIT.

3 Phase Analysis

The betatron phase ϕ is related to β by the standard equation

$$\frac{d\phi}{ds} = \frac{1}{\beta} \, . \tag{27}$$

Taking the variation of both sides gives

$$\frac{d\delta\phi}{ds} = \frac{-\delta\beta}{\beta^2} \, . \tag{28}$$

Using Eqs. (27) and (28) with Eq. (22), and using the added boundary condition that $\delta\phi(s_k) = 0$ gives

$$\delta\phi(s) = \begin{cases} 0 & s < s_k \\ \frac{\beta_k \delta k \, l}{2}(\cos 2(\phi(s) - \phi_k) - 1) & s > s_k \end{cases} \, . \tag{29}$$

A free phase wave looks similar to a free beta wave but with an offset. The fit to the A and B regions is thus

$$\delta\phi(s) = \begin{cases} \lambda_a \, \sin 2\phi(s) + \rho_a \, \cos 2\phi(s) + C_a & s < s_k \\ \lambda_b \, \sin 2\phi(s) + \rho_b \, \cos 2\phi(s) + C_b & s > s_k \end{cases} \, . \tag{30}$$

Going to a new reference so that the variation $\delta\tilde{\phi}$ with respect to the new reference is zero for $s < s_k$ gives

$$\delta\tilde{\phi}(s) = \begin{cases} 0 & s < s_k \\ \lambda_{ba} \, \sin 2\phi(s) + \rho_{ba} \, \cos 2\phi(s) + C_{ba} & s > s_k \end{cases} \, . \tag{31}$$

where λ_{ba} and ρ_{ba} are defined by Eqs. (4) and

$$C_{ba} \equiv C_b - C_a \, . \tag{32}$$

Comparing Eq. (29) with Eq. (31) the fit variables should obey the relationship

$$|C_{ba}| = A_{ba} \, , \tag{33}$$

where A_{ba} is defined by Eq. (8). In actuality, the presence of multiple quadrupole errors or errors in the measurement itself will make the fitted values not obey Eq. (33). We can thus define a figure of merit χ_A by

$$\chi_A \equiv \frac{\Big| |C_{ba}| - A_{ba} \Big|}{|C_{ba}| + A_{ba}} \, . \tag{34}$$

The condition necessary for the analysis to be valid is

$$\chi_A \ll 1 \, . \tag{35}$$

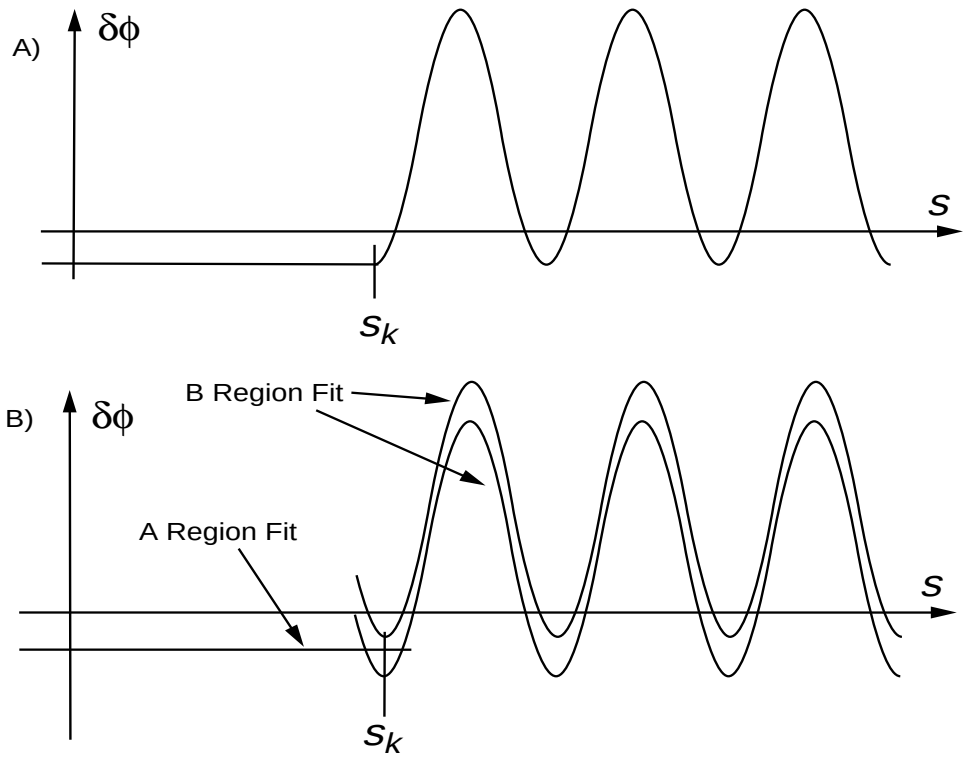

Figure 3: (a) In theory $\delta\phi(s)$ is continuous and has a continuous derivative. (b) In practice the fits to the A and B regions will fail to intersect or intersect with a discontinuous derivative. The best guess for the location of the kick is where the derivatives match. [Note: For illustration purposes the A region fit is taken to be a straight line.]

In theory, at s_k (or any other point) $\delta\phi(s)$ is continuous and has a continuous derivative as shown in figure 3(a). In actuality, because Eq. (33) is not exactly satisfied, the fit will produce a situation as shown in figure 3(b) where the free waves do not intersect or intersect with a discontinuous derivative. The best solution is to choose for s_k the point where the derivatives match as shown in figure 3(b). Using this criterion with Eqs. (29) and (31) gives for ϕ_k

$$\sin 2\phi_k = \frac{-\lambda_{ba}\,\mathrm{sgn}C_{ba}}{A_{ba}}\,,$$
$$\cos 2\phi_k = \frac{-\rho_{ba}\,\mathrm{sgn}C_{ba}}{A_{ba}}\,. \tag{36}$$

where

$$\mathrm{sgn}C_{ba} \equiv \begin{cases} 1 & C_{ba} > 0 \\ -1 & C_{ba} < 0 \end{cases} \tag{37}$$

Eqs. (36) has solutions spaced π apart. Comparing Eq. (29) with Eq. (31) gives two equations for the magnitude of the kick

$$\beta_k \delta k \, l = -2C_{ba} \, , \tag{38}$$

and

$$\beta_k \delta k \, l = 2(\lambda_{ba} \, \sin 2\phi_k + \rho_{ba} \, \cos 2\phi_k) \, . \tag{39}$$

Since Eq. (33) is not in general obeyed Eqs. (38) and (39) will not give the same answer. In K_FIT the average of the two is taken.

Figure 4 shows an example analysis of vertical phase data that was taken by Stu Henderson et. al. because the tune was seen to aperiodically jump. To extend the data past L0 the formula

$$\delta\phi(s + s_{ring}) = \delta\phi(s) + \delta\phi(s_{ring}) \tag{40}$$

is used where $\delta\phi(s_{ring})$ is the difference in tune between the data and the reference. σ_a/A_a and σ_b/A_b are computed from Eq. (9). The relative uncertainty in the kick σ_K/K is calculated in analogy from Eq. (12)

$$\frac{\sigma_K}{K} = \frac{\sqrt{\lambda_{ba}^2 \sigma_{\lambda ba}^2 + \rho_{ba}^2 \sigma_{\rho ba}^2 + C_{ba}^2 \sigma_{Cba}^2}}{\lambda_{ba} \, \sin 2\phi_k + \rho_{ba} \, \cos 2\phi_k - C_{ba}} \, . \tag{41}$$

The uncertainty in ϕ_k is computed from Eq. (14).

A quadrupole error is readily apparent and the phase at the kick shows it to be quadrupole Q31E. This was verified using the program QSTST. The tune jump problem was solved by changing the controller card. Analysis of the the horizontal phase data (not shown) also shows an error at Q31E as expected. Note that K_FIT follows the convention that irregardless of the plane being analyzed, a positive δk means the error horizontally focuses and vertically defocuses.

4 Coupling Analysis

The 4×4 transfer matrix for a thin skew quad error is[4]

$$\mathbf{T}_{\rm err} = \begin{pmatrix} \mathbf{1} & \mathbf{q} \\ \mathbf{q} & \mathbf{1} \end{pmatrix} \, , \tag{42}$$

where

$$\mathbf{q} = \begin{pmatrix} 0 & 0 \\ \delta q & 0 \end{pmatrix} \, , \tag{43}$$

with δq being the strength of the error. To first order any 1-turn transfer matrix can be written as (Sagan and Rubin[4] Eq. (33))

$$\mathbf{T} = \begin{pmatrix} \mathbf{A} & \mathbf{CB - AC} \\ \mathbf{BC^+ - C^+A} & \mathbf{B} \end{pmatrix} \tag{44}$$

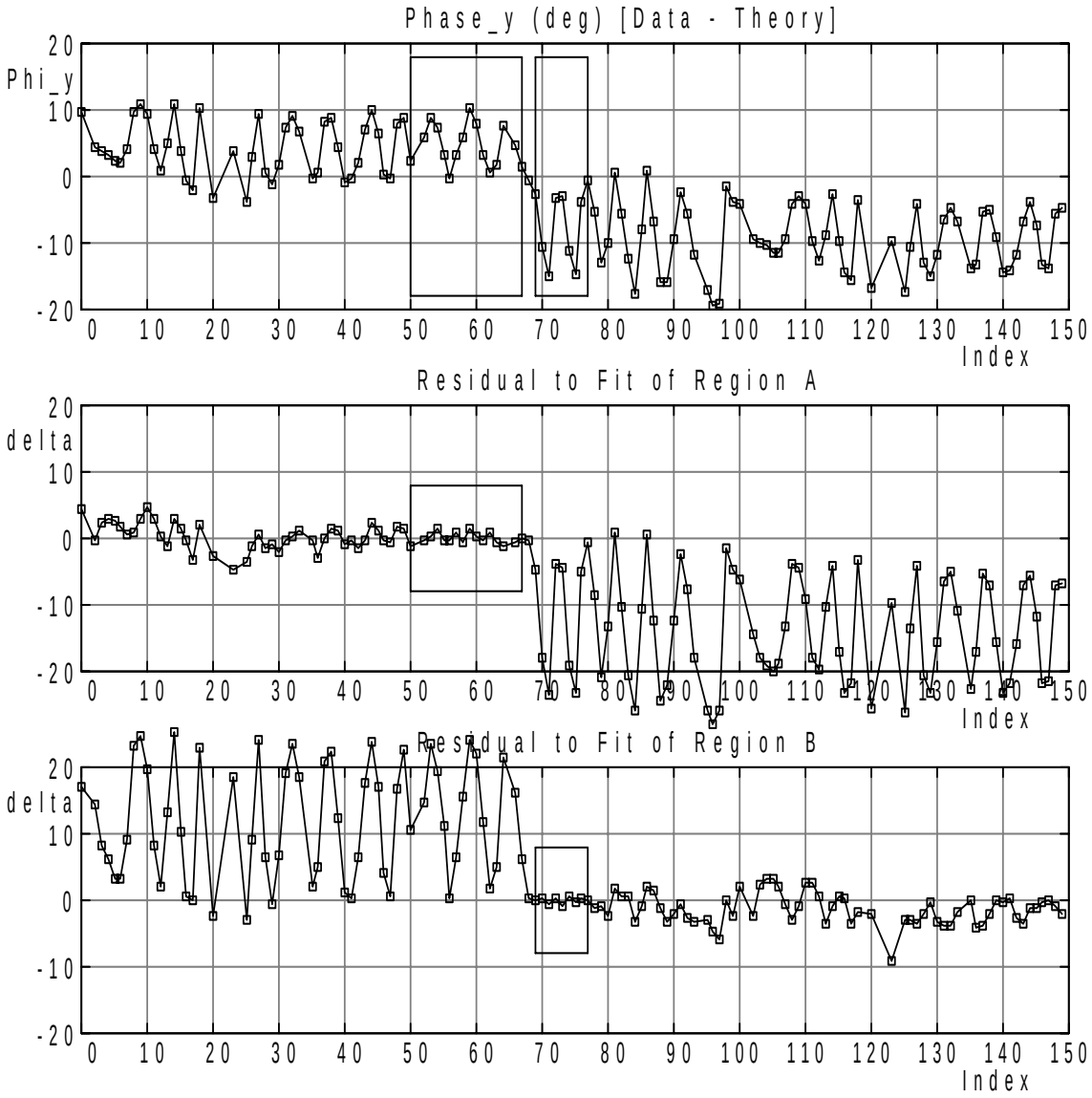

Figure 4: Wave analysis of vertical phase data

We take the boundary condition to be $\mathbf{C}(s) = \mathbf{0}$ for $s < s_k$. Thus at a point s_{k-} just before the error the 1-turn matrix $\mathbf{T}_{k-}$ is

$$\mathbf{T}_{k-} = \begin{pmatrix} \mathbf{A} & \mathbf{0} \\ \mathbf{0} & \mathbf{B} \end{pmatrix} \tag{45}$$

The 1-turn matrix $\mathbf{T}_{k+}$ just after the error is then to first order

$$\begin{aligned} \mathbf{T}_{k+} &= \mathbf{T}_{\rm err}\, \mathbf{T}_{k-}\, \mathbf{T}_{\rm err}^{-1} \\ &= \begin{pmatrix} \mathbf{A} & \mathbf{qB} - \mathbf{Aq} \\ -\mathbf{Bq} + \mathbf{qA} & \mathbf{B} \end{pmatrix} \end{aligned} \tag{46}$$

Comparing Eq. (44) with Eq. (46) gives

$$\mathbf{C}(s_{k+}) = \mathbf{q}\,. \tag{47}$$

Converting $\mathbf{C}$ to $\overline{\mathbf{C}}$ (Cf. Bagley and Rubin[5]) gives

$$\overline{\mathbf{C}}(s_{k+}) = \begin{pmatrix} 0 & 0 \\ \delta\bar{q} & 0 \end{pmatrix}\,, \tag{48}$$

where $\delta\bar{q} = \sqrt{\beta_x \beta_y}\, q$. If the error is due to a variation in strength then $\delta\bar{q}$ is given by[4]

$$\delta\bar{q} = -\sqrt{\beta_x(s_k)\beta_y(s_k)}\, \delta k\, l\, \sin 2\theta_q\,, \tag{49}$$

where θ_q is the rotation angle of the quad with $\theta_q = 0$ being an upright (non–skew) quad. Alternatively, if the error is due to a variation in rotation angle $\delta\theta_q$ then

$$\delta\bar{q} = -2\sqrt{\beta_x(s_k)\beta_y(s_k)}\, k \delta\theta_q \cos 2\theta_q\,. \tag{50}$$

For $s > s_k$, $\overline{\mathbf{C}}(s)$ propagates as given by Sagan and Rubin[4] Eq. (22). The solution is thus

$$\overline{\mathbf{C}}(s) = \begin{cases} 0 & s < s_k \\ \frac{\delta\bar{q}}{2}\left[\mathbf{S}\left(\frac{\pi}{2} - \phi_+(s) + \phi_+(s_k)\right) - \mathbf{R}\left(\frac{\pi}{2} + \phi_-(s) - \phi_-(s_k)\right)\right] & s > s_k \end{cases}\,, \tag{51}$$

where $\mathbf{S}$ and $\mathbf{R}$ are the rotational and anti-rotational matrices

$$\begin{aligned} \mathbf{R}(\theta) &= \begin{pmatrix} \cos\theta & \sin\theta \\ -\sin\theta & \cos\theta \end{pmatrix}\,, \\ \mathbf{S}(\phi) &\equiv \begin{pmatrix} \cos\phi & \sin\phi \\ \sin\phi & -\cos\phi \end{pmatrix}\,, \end{aligned} \tag{52}$$

and

$$\begin{aligned} \phi_+ &\equiv \phi_x + \phi_y\,, \\ \phi_- &\equiv \phi_x - \phi_y\,. \end{aligned} \tag{53}$$

The $\overline{\mathbf{C}}$ free wave has components that propagate as the sum and difference of the phases. The formula for the fit to the A and B regions for any of the $\overline{\mathbf{C}}$ matrix elements is thus

$$\overline{C}_{ij}(s) = \begin{cases} \lambda_{a,ij}\,\sin\phi_+(s) + \rho_{a,ij}\,\cos\phi_+(s) + \gamma_{a,ij}\sin\phi_-(s) + \zeta_{a,ij}\cos\phi_-(s) & s < s_k \\ \lambda_{b,ij}\,\sin\phi_+(s) + \rho_{b,ij}\,\cos\phi_+(s) + \gamma_{b,ij}\sin\phi_-(s) + \zeta_{b,ij}\cos\phi_-(s) & s > s_k \end{cases} \tag{54}$$

going to a new reference such that the normalized coupling $\tilde{C}(s)$ with respect to the new reference is zero for $s < s_k$ gives[†]

$$\tilde{C}(s) = \begin{cases} 0 & s < s_k \\ \lambda_{ba}\sin\phi_+(s) + \rho_{ba}\cos\phi_+(s) + \gamma_{ba}\sin\phi_-(s) + \zeta_{ba}\cos\phi_-(s) & s > s_k \end{cases} \tag{55}$$

with λ_{ba} and ρ_{ba} defined by Eqs. (4) and

$$\begin{aligned} \gamma_{ba} &\equiv \gamma_b - \gamma_a\ , \\ \zeta_{ba} &\equiv \zeta_b - \zeta_a\ . \end{aligned} \tag{56}$$

The phase at the error is found by comparing Eq. (51) with Eq. (55)

$$\tan\phi_+(s_k) = \frac{-\rho_{ba,11}}{\lambda_{ba,11}} = \frac{\lambda_{ba,12}}{\rho_{ba,12}} = \frac{-\rho_{ba,22}}{\lambda_{ba,22}} \tag{57}$$

and

$$\tan\phi_-(s_k) = \frac{-\zeta_{ba,11}}{\gamma_{ba,11}} = \frac{\gamma_{ba,12}}{\zeta_{ba,12}} = \frac{-\zeta_{ba,22}}{\gamma_{ba,22}} \tag{58}$$

The magnitude of the kick is given by

$$\begin{aligned} \frac{\delta\bar{q}}{2} &= \lambda_{ba,11}\cos\phi_+(s_k) - \rho_{ba,11}\sin\phi_+(s_k) \\ &= \lambda_{ba,12}\sin\phi_+(s_k) + \rho_{ba,12}\cos\phi_+(s_k) \\ &= -\lambda_{ba,22}\cos\phi_+(s_k) + \rho_{ba,22}\sin\phi_+(s_k) \end{aligned} \tag{59}$$

and

$$\begin{aligned} \frac{\delta\bar{q}}{2} &= \gamma_{ba,11}\cos\phi_-(s_k) - \zeta_{ba,11}\sin\phi_-(s_k) \\ &= -\gamma_{ba,12}\sin\phi_-(s_k) - \zeta_{ba,12}\cos\phi_-(s_k) \\ &= \gamma_{ba,22}\cos\phi_-(s_k) - \zeta_{ba,22}\sin\phi_-(s_k) \end{aligned} \tag{60}$$

[The 21 component is ignored since it cannot be measured at present.]

Comparing Eq. (51) with Eq. (55) we find the condition that

$$A_{s,ba} = A_{r,ba}\ , \tag{61}$$

[†]For compactness ij indices are dropped from this equation and in equations below except where necessary

where

$$A_{s,ba}^2 \equiv \lambda_{ba}^2 + \rho_{ba}^2 \,,$$
$$A_{r,ba}^2 \equiv \gamma_{ba}^2 + \zeta_{ba}^2 \,. \tag{62}$$

Similar to the phase analysis Eq. (61) will, in practice, not be obeyed exactly by the fitted values. we can thus define a figure of merit χ_A by

$$\chi_A \equiv \frac{|A_{s,ba} - A_{r,ba}|}{A_{s,ba} + A_{r,ba}} \,, \tag{63}$$

We would like

$$\chi_A \ll 1 \,. \tag{64}$$

however, even if condition (64) is violated, it is possible to do a good analysis. This is true since the variation of $\phi_-(s)$ as a function of s is small compared to the variation of $\phi_+(s)$. It is thus possible to do a poor job of fitting γ and ζ while doing a good job of fitting λ and ρ. Since λ and ρ alone will give $\phi_+(s_k)$ and $\delta\bar{q}$, this is good enough to pinpoint the error.

Figures of merit for the fits, $\sigma_{s,a}/A_{s,a}$, $\sigma_{r,a}/A_{r,a}$, $\sigma_{s,b}/A_{s,b}$, and $\sigma_{r,b}/A_{r,b}$ can also be defined

$$\frac{\sigma_s}{A_s} \equiv \frac{\sqrt{\sigma_\lambda^2 + \sigma_\rho^2}}{A_s} \,,$$
$$\frac{\sigma_r}{A_r} \equiv \frac{\sqrt{\sigma_\gamma^2 + \sigma_\zeta^2}}{A_r} \,,$$
$$, \tag{65}$$

with $A_{s,a}$, $A_{s,b}$, $A_{r,a}$ and $A_{r,b}$ being defined in an analogous manner to Eq. (62). Finally, The relative uncertainty of the kick magnitude $\sigma_{K,s}/K_s$ and $\sigma_{K,r}/K_r$ is given by

$$\frac{\sigma_{K,s}}{K_s} = \frac{\sqrt{\lambda_{ba}^2 \sigma_{\lambda ba}^2 + \rho_{ba}^2 \sigma_{\rho ba}^2}}{A_{s,ba}} \,,$$
$$\frac{\sigma_{K,r}}{K_r} = \frac{\sqrt{\gamma_{ba}^2 \sigma_{\gamma ba}^2 + \zeta_{ba}^2 \sigma_{\zeta ba}^2}}{A_{r,ba}} \,, \tag{66}$$

and the uncertainty in the phase at the kick is

$$\sigma_{\phi+} = \frac{\sqrt{\rho_{ba}^2 \sigma_{\lambda ba}^2 + \lambda_{ba}^2 \sigma_{\rho ba}^2}}{A_{s,ba}} \,,$$
$$\sigma_{\phi-} = \frac{\sqrt{\zeta_{ba}^2 \sigma_{\gamma ba}^2 + \gamma_{ba}^2 \sigma_{\zeta ba}^2}}{A_{r,ba}} \,. \tag{67}$$

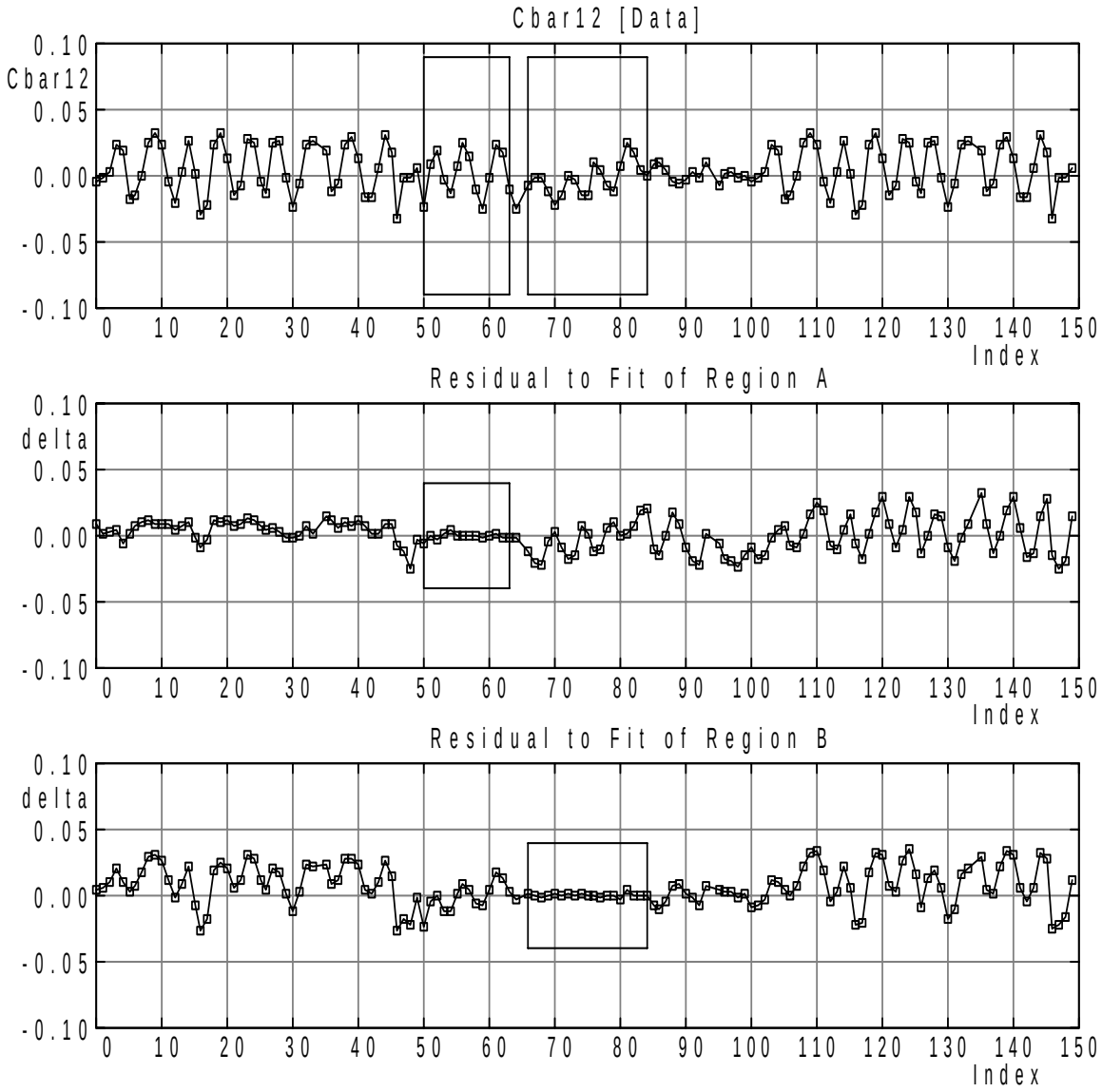

A Region: Sig_s/A_s: 0.056 Sig_r/A_r: 0.895
B Region: Sig_s/A_s: 0.059 Sig_r/A_r: 0.066
Chi_A: 0.064
Kick Sig_Ks/Ks: 0.092 Sig_Kr/Kr: 0.107
Kick Sig_phi+: 0.092 Sig_phi-: 0.109

After Det# kick phi_+ phi_- phi_x phi_y
63 0.0235 82.707 6.527 44.617 38.090

26-NOV-96 07:53:26
N9A19C501.FD93S_4S
[CESR.PHASE.WAVE]
Dat: H2_CBAR.DAT;2
Ref: NONE
CESR Set: 42743

IX_A1, IX_A2: 50 63
IX_B1, IX_B2: 66 84

Figure 5: Wave analysis of $\overline{C}_{12}$.

Figure 5 shows an analysis of $\overline{C}_{12}$ data taken by Dave Rubin and Sasha Temnykh. The fit to the regions is good despite the large $\sigma_{r,a}/A_{r,a}$ which is due to a small value for $A_{r,a}$. The kick is seen to be between detectors 63 and 64. The calulated values for $\phi_x(s_k)$ and $\phi_y(s_k)$ are calculated from the calulated values of $\phi_+(s_k)$ and $\phi_-(s_k)$ and Eqs. (53). The best candidates for the source of the kick error is the horizontal steering H36E or the bend B36E. the steering and bend are at a phase $\phi_x(H/B36E) = 44.347$ and $\phi_y(H/B36E) = 38.258$. H36E had a strength of -1419 CU during the measurement. Because of possible problems with the calculation of γ and ζ the kick magnitude is given using Eq. (59).

5 Acknowledgements

My thanks to Mike Billing in particular for useful discussions and to members of the operations group in general for providing the data.

References

[1] C. Bovet, R. Gouiran, I. Gumowski, and K. H. Reich, "A Selection of Formulae and Data Useful for the Design of A. G. Synchrotrons," CERN/MPS-SI/Int. DL/70/4 (1970).

[2] Matthew Sands, *The Physics of Electron Storage Rings, An Introduction*, SLAC-121 Addendum. (1970).

[3] W. Press, B. Flannery, S. Teukolsky, and W. Wetterling, *Numerical Recipes in Fortran, the Art of Scientific Computing*, Second Edition, Cambridge University Press, New York, 1992.

[4] D. Sagan and D. Rubin, "Propagation of Twiss and Coupling Parameters," Cornell CBN 96-20, 1996.

[5] P. Bagley and D. Rubin, "Correction of Transverse Coupling in a Storage Ring," Proc. 1989 Part. Acc. Conf. (San Francisco) p. 874, (1989).